AAEC - PR - 80-82

AAEC/PR80-82
(extract)

AAEC/PR80-82
(extract)

AUSTRALIAN ATOMIC ENERGY COMMISSION

RESEARCH ESTABLISHMENT

LUCAS HEIGHTS RESEARCH LABORATORIES

PROGRESS REPORT

FOR

MATERIALS DIVISION

1 JULY 1981 - 30 JUNE 1982

Chief: Dr P.M. Kelly

PROGRESS REPORT

FOR

MATERIALS DIVISION

1 JULY 1981 - 30 JUNE 1982

Chief: Dr P.M. Kelly

FOREWORD

During this period, there was a major reorganisation of the AAEC. Research projects on acoustic emission and hydrogen production and storage were transferred to CSIRO, and research on the laser enrichment of isotopes was taken over by the Division.

The Division's research program has centred on SYNROC research and development, high strength steels, fusion reactor materials, and non-destructive testing. In addition, the Division has again provided a number of services to industry and other outside organisations and to other parts of the AAEC.

During the year, Mr Mohd bin Harun, Mr Abdul Aziz Mohamed and Mr Pauzi Ismail from the Tun Ismail Atomic Research Centre (Puspati, Malaysia) were attached to the Division for training and practical experience.

CONTENTS

1. MATERIALS SCIENCE SECTION

(Leader: C.J. Ball)

1.1 Maraging Steels

(J.T.A. Pollock*, R. Clissold*, E. Meller, R. Warren, K.G. Watson, B. Zybenko, C.J. Ball, R.G. Blake)

1.1.1 Thermal embrittlement

Maraging steels combine very high strength with high toughness and so are candidate materials for the construction of centrifuge rotors. However, it has been known for some time that they are subject to thermal embrittlement if incorrectly heat treated. This has been attributed to the precipitation of TiC at prior austenite grain boundaries, but the effect of varying the levels of carbon and other residual impurities on the degree of embrittlement has not been investigated previously.

The thermal embrittlement of two casts of fully age-hardened MAR350 with different levels of residual elements was investigated, using fracture toughness measurements, microstructural studies and X-ray diffraction of the extracted precipitates. These were supplied as seamless, hot extruded and annealed tubes of 13 mm wall thickness. Compositions are listed in Table 1.

TABLE 1
CHEMICAL COMPOSITION OF MAR350 STEELS

	Element (wt %)								
Type	C	S	P	Si	Mn	Ni	Ti	Mo	Co
Steel A	0.0006	0.008	0.005	0.07	0.04	17.8	1.5	4.2	11.8
Steel B	0.003	0.003	0.004	0.02	0.02	17.8	1.5	3.7	12.4

After cutting and flattening the tubes in a press, single edge notch specimens were machined from the slabs according to ASTM specifications. The specimens were solution treated for 1 h at 1470 K, transferred *in vacuo* to a second furnace at 1175 K and held at this temperature for 2 to 200 min before quenching in oil. Fracture toughness samples were fatigue cracked under cyclic loading before ageing for 3 h at 760 K, since controlled cracking of aged MAR350 is difficult. The toughness value measured is not a true K_{IC}

* Now with CSIRO

value according to ASTM procedures since the crack was introduced before the completion of heat treatment. Three or more K_{IC} measurements were made for each heat treatment.

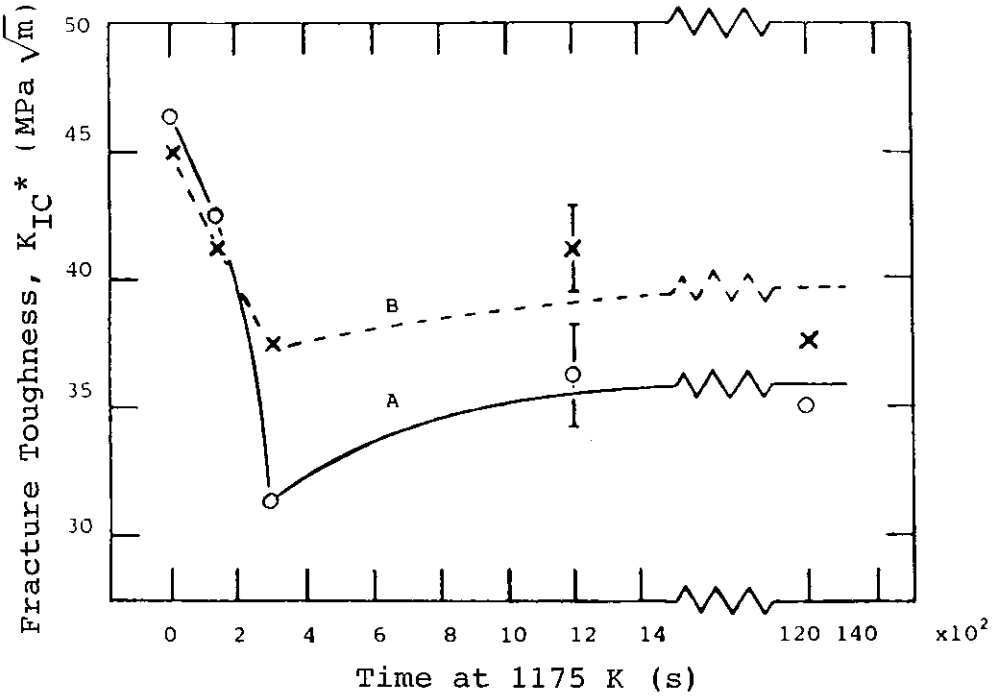

FIGURE 1. VARIATION OF FRACTURE TOUGHNESS WITH TIME AT 1175 K

The variation of fracture toughness with time at 1175 K is shown in Figure 1, together with an average error bar for each steel. These results illustrate the following significant features:

(i) In the unsensitised condition, fracture toughness is independent of the amount of residual impurities, within the range investigated.

(ii) After as little as five minutes at 1175 K, there is a substantial reduction in toughness for both steels.

(iii) The reduction in toughness is greater for the steel having the larger residual impurities.

(iv) There is some recovery of toughness in steel A if the time at 1175 K is extended beyond 300 s.

Scanning electron microscopy of fracture surfaces in aged samples showed that before sensitising, fracture occurred by transgranular cleavage. When the time at 1175 K was extended, there was a subtle change in the appearance

of the fracture surfaces. The average size of the cleavage planes was reduced, the fracture surface assumed a 'chunkier' appearance and the general outline of the prior γ grains began to emerge.

Changes in the appearance of fracture surfaces in unaged samples (i.e. without the 3 hour anneal at 760 K) was much more dramatic. After two minutes at 1175 K, there was a transition from dimpled transgranular to severe intercrystalline failure. The ratio of intercrystalline to transgranular fracture increased with time at 1175 K. However, although the prior γ grain boundaries were followed, each face had fractured by a mixture of cleavage and ductile tearing, a phenomenon best described as quasi-cleavage.

Optical microscopy showed extensive precipitation on prior γ grain boundaries. Electron microscopy of carbon extraction replicas from overpolished surfaces showed that after short times at 1175 K, the precipitate had a dendritic or featherlike form. The feathery precipitate was not observed after 20 or 200 minutes at 1175 K. Kikuchi patterns from this precipitate showed that it was cubic, with a lattice parameter of (0.4338 ± 0.0015 nm), and identifiable as TiC. Some large precipitates were also observed in all fracture surfaces. Energy-dispersive X-ray analysis (EDX) showed that they contained titanium and sulphur and presumably were Ti_2S or $Ti_4C_2S_2$; we cannot detect carbon by EDX analysis. These particles did not appear to contribute to grain boundary weakening.

The precipitate was extracted by the electrolytic disolution of unaged samples and X-ray photographs were taken using a Debye-Scherrer camera. Unfortunately, the extraction was not quantitative so only relative amounts of the different precipitates could be determined. All specimens contained TiN and $Ti_4C_2S_2$ (or Ti_2S), and specimens that had been sensitised at 1175 K also contained TiC. The proportion of TiC and, to a lesser extent, $Ti_4C_2S_2$ increased with time at 1175 K, in agreement with the observation that TiC precipitates on the γ grain boundaries during sensitisation at 1175 K. The stabilisation or recovery of fracture toughness with prolonged holding at 1175 K, despite a continuing increase in the proportion of TiC extracted from the sample, is presumably related to the change in morphology of the grain-boundary precipitate.

The dependence of embrittlement on the level of residual impurities, of which carbon is presumably the most important, together with the fact that carbon may be bound in the form of $Ti_4C_2S_2$, suggests that it may be possible

to control susceptibility to embrittlement by heat treatment. This is being investigated.

1.2 Martensite Crystallography

(P.M. Kelly, R.G. Blake, C.J. Ball, J.N. Winning)

Work continued on the crystallography of martensitic transformations, using an Fe-Ni-Mn alloy. This alloy transforms isothermally at temperatures of $\sim$ -70°C so it is possible to prepare specimens with substantial amounts of retained austenite, thus enabling very precise measurements of the orientation relation between austenite and martensite to be made. The results were in good agreement with those of other alloys that transform to lath martensite; this is explained by a lattice invariant deformation caused by shear on the $(\bar{1}21)[11\bar{1}]$ and $(12\bar{1})[\bar{1}11]$ systems in the martensite. Attempts are being made to measure the habit plane and shape deformation to provide a further check on the theory.

An attempt was also made to understand an alternative theory of martensitic transformations. It was found that this theory violates the law of conservation of matter, and so can be discarded.

1.3 Laser Enrichment

1.3.1 Laser photophysics

(J.W. Kelly, H. Struve, N. Hamilton)

The Laser Photophysics Group is studying the chemical reactions induced on large polyatomic molecules by short, microsecond pulses of CO_2 laser irradiation. Part of this work involves the evolution of a technique capable of fast, direct monitoring of the initial phases of these reactions. Present work is based on the use of a very sensitive infrared detector and advanced computer-based data handling techniques.

The group is also responsible for monitoring overseas developments in laser isotopic separation (LIS) processes for uranium enrichment. It has noted the recent major advances in copper laser development, fundamental to the preferred atomic vapour LIS process, and major advances in the development of 16 μm lasers for the molecular LIS, UF_6 process, by the use of CO_2 lasers and Raman shifting. Proponents of both processes claim enrichment costs of about a quarter of that of centrifuge/diffusion plants.

1.4 Techniques

1.4.1 Microanalysis

(R.G. Blake, R.B. Warren, C.J. Ball, G.T. Kane)

Difficulties are still being experienced with microanalysis in the JSEM-200 electron microscope. The cause of the problem is the position of the detector, which is in the same horizontal plane as the specimen and directed at 45° to the axis of tilt of the specimen holder. To avoid shadowing the X-rays emitted by the specimen, the specimen holder must be tilted to face the detector; this requires rotations about two axes. It is also necessary not to intercept the electron beam with the specimen holder. The main source of extraneous X-rays was the specimen holder which has since been replaced with a beryllium holder. Progress has generally been slow because the EDX equipment (Tracor Northern, TM1710) must be shared with the JSM-U3 scanning electron microscope; lately, work has come to a halt because of a leak in the window of the solid state detector.

1.4.2 Image analysis

(J.G. Napier, P.M. Kelly)

The quantitative image analyser has been developed to the point where it is possible to acquire, store, recover and print images using sixteen grey levels, and to manipulate these images in a variety of ways, e.g. suppress or enhance contrast over a specified range of levels, invert, etc. The system aroused considerable interest at the Seventh Australian Conference on Electron Microscopy (Canberra, February 1982), where it was on display. Software for the analysis of images is being developed. The information sought includes the number of particles within the field of view, in total or within a specified range of brightness, the distribution of areas of these particles, their shapes, etc. One problem that has arisen is that the TV camera doe not evenly illuminate the whole of the field of view, so particles which would be brighter than a specified level if in the centre of the field of view do not reach this level of brightness if situated near the margins; this introduces errors into quantitative phase analysis. We are endeavouring to obtain a better camera.

1.4.3 X-ray diffraction

(R.B. Warren, C. Hall, G.T. Kane, C.J. Ball)

The high temperature X-ray camera has been overhauled and the associated horizontal X-ray tube arranged to operate from the PW1010 generator. The control circuitry of this generator has been replaced by a solid state module which is performing satisfactorily.

A recirculating water-cooling system was installed to eliminate problems arising from transient drops in mains water pressure.

A technique has been developed to enable back-reflection X-ray photographs to be taken from precisely determined areas of a specimen, using a 100 μm diameter beam.

1.4.4 Metallography

(E. Meller, C. Hall, J.N. Winning)

During the year, a precision diamond saw and improved specimen mounting equipment were obtained.

1.5 Service Work

1.5.1 Scanning electron microscopy

(K.G. Watson, J.N. Winning)

The bulk of the scanning electron microscopy work continues to be for the SYNROC project. Other work has included microscopy of fracture surfaces in maraging steel, analysis of precipitates in these fracture surfaces and assisting the Commonwealth Police with a forensic investigation.

1.5.2 Metallography

(E. Meller, C. Hall, R.B. Warren, J.N. Winning)

Routine service work and consultative failure analysis has been carried out for the Division and CEPD. Much of the work has been on maraging steels and SYNROC, but stainless steels, carbon fibre composites and asbestos-based materials have also been examined.

1.5.3 Data processing

(J.G. Napier)

The data processing program written for stores control has been expanded to handle allocation of staff effort to projects as well, and has been implemented for AM and C and Applied Physics Divisions.

2. MATERIALS PERFORMANCE

(Leader, K.U. Snowden)

2.1 Introduction

In-service, structural materials are often required to withstand long-term steady or fluctuating stresses that occur frequently over a range of temperatures and in corrosive environments. These types of stress and environmental conditions are important because they are likely to restrict severely the service life of the structure. Work on fatigue, creep and the application of fracture mechanics to different types of failure has continued with studies of austenitic and ferritic steels and refractory metals.

2.2 Fatigue Crack Growth and Cyclic Plastic Zone Size

A comparison was made of the fatigue crack growth rates at room temperature in type 321 stainless steel formed into 1 mm thick SEN tension specimens and 10 mm thick SEN bending specimens. Comparisons were also made between the fatigue crack growth rates in 1 mm thick SEN tension specimens, made from type 310 stainless steel and type A533B pressure vessel steel, and the rates reported in the literature for thicker specimens of these materials. These comparisons showed that, at low values of the stress intensity range, ΔK, there was little difference between the rates in thick and thin specimens. However, at high ΔK, the fatigue crack growth rates were up to an order of magnitude lower in the thin specimens than in the thick specimens (Figure 2).

Micro-hardness measurement surveys around crack tips in specimens of type 321 stainless steel revealed that the cyclic plastic zone size was proportional to $(\Delta K)^n$, where $n \cong 2$ for the SEN bending (B = 10 mm) specimens and $\cong 0.5$ for the SEN tension (B = 1 mm) specimens. The fatigue crack growth rate behaviour of the thick and thin specimens was also reflected in the size of the cyclic plastic zone; at $\Delta K \geq 17$ MPa $\sqrt{m}$, the cyclic plastic zone size in the thin specimens was less than that in thick specimens at the same ΔK. Further, da/dN was approximately proportional to (cyclic plastic zone

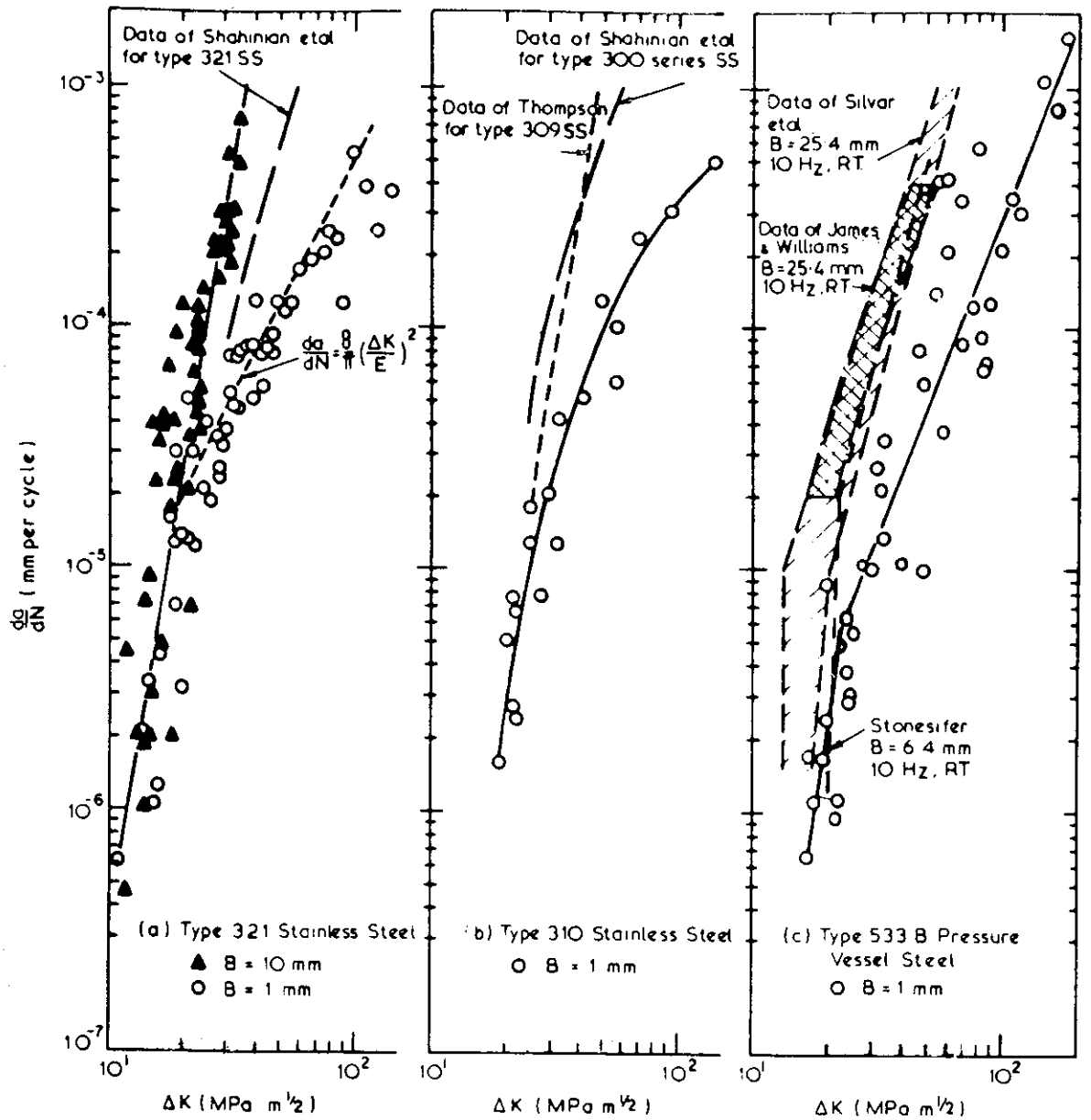

Figure 2 (a) Crack growth rates for type 321 stainless steel SEN tension (B = 1 mm) specimens, open points; and SEN bending (B = 10 mm) specimens, closed points. A dashed line represents the equation $da/dN = (8/\pi)\ (\Delta K/E)^2$.
(b) Crack growth rates for type 310 stainless steel SEN tension (B = 1 mm) specimens. The dashed curve represents Thompson's data for type 309S stainless steel specimens with B = 7.5 mm, and the dotted curve represents the composite data of Shahinian et al. for type 300 series stainless steels with B = 12.7 mm.
(c) Crack growth rates for type A533B pressure vessel steel SEN tension (B = 1 mm) specimens. The dashed and dotted curves are taken from references for the same steel with B = 5.08 to 25.4 mm.

size)$^{3.5}$, a relationship which appeared to be independent of thickness.

Scanning electron microscopy of the cyclic plastic zone at the crack tip revealed a grid of coarse slip lines which were consistent with those expected from a shear-sliding mechanism for crack growth (Figures 3a and b). This experiment predicted crack growth rates that were in agreement with those in the SEN tension specimens of type 321 stainless steel at $\Delta K \geq 17$ MPa $\sqrt{m}$.

The values of ΔK at which deviations in the da/dN - ΔK curves for thick and thin specimens occurred were compared with the limitations imposed by three different size criteria. The criterion which gave the best agreement limited the cyclic plastic zone size to $\sim$ 3 per cent of the uncracked ligament.

2.3 Fatigue of Refractory Metals

The fatigue life of the refractory metals tantalum, molybdenum and niobium was measured over the temperature range 20 to 750°C. The tests were done at a frequency of 16 Hz and a strain range of ± 0.2 per cent in cantilever bending *in vacuo*. The results are shown in Figure 4.

The main points of interest are as follows:

- The fatigue life at room temperature is approximately the same for each metal.
- For niobium, the fatigue life increases as the temperature is raised above room temperature and remains approximately constant between 200 and 750°C.
- For tantalum and molybdenum, the fatigue life decreases as the temperature is raised above room temperature.
- Tantalum shows a minimum in fatigue life at about 600°C; the life then increases as the temperature is raised above 600°C.
- Molybdenum shows no changes in fatigue life in the range 150 to 500°C then it decreases as the temperature increases.

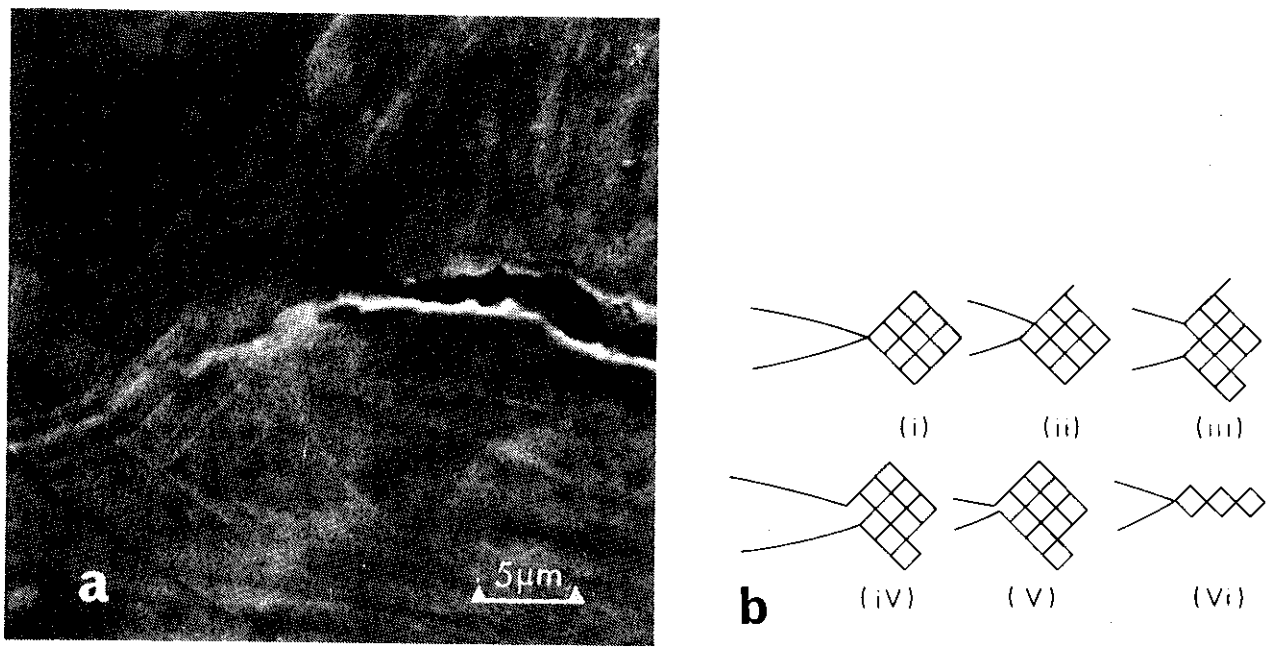

Figure 3 (a) Area around crack tip in type 321 stainless steel SEN tension (B = 1 mm) specimens, ΔK = 20 MPa $\sqrt{m}$. Area shows grid of coarse slip lines.
(b) Geometric model of fatigue-crack growth by shear sliding (Laird-Smith-Neumann model). (i) Initial configuration. (ii) Crack opened in tension with shear sliding on one slip plane above the crack plane. (iii) Followed by shear sliding on one slip plane below the crack plane. (iv) Crack unloaded with reversed shear sliding on slip plane of (ii). (v) Followed by reversed shear sliding on slip plane of (iii); the crack as advanced. (vi) After a number of repetitions of the mechanism; note that fatigue striations have been formed. After Weertman

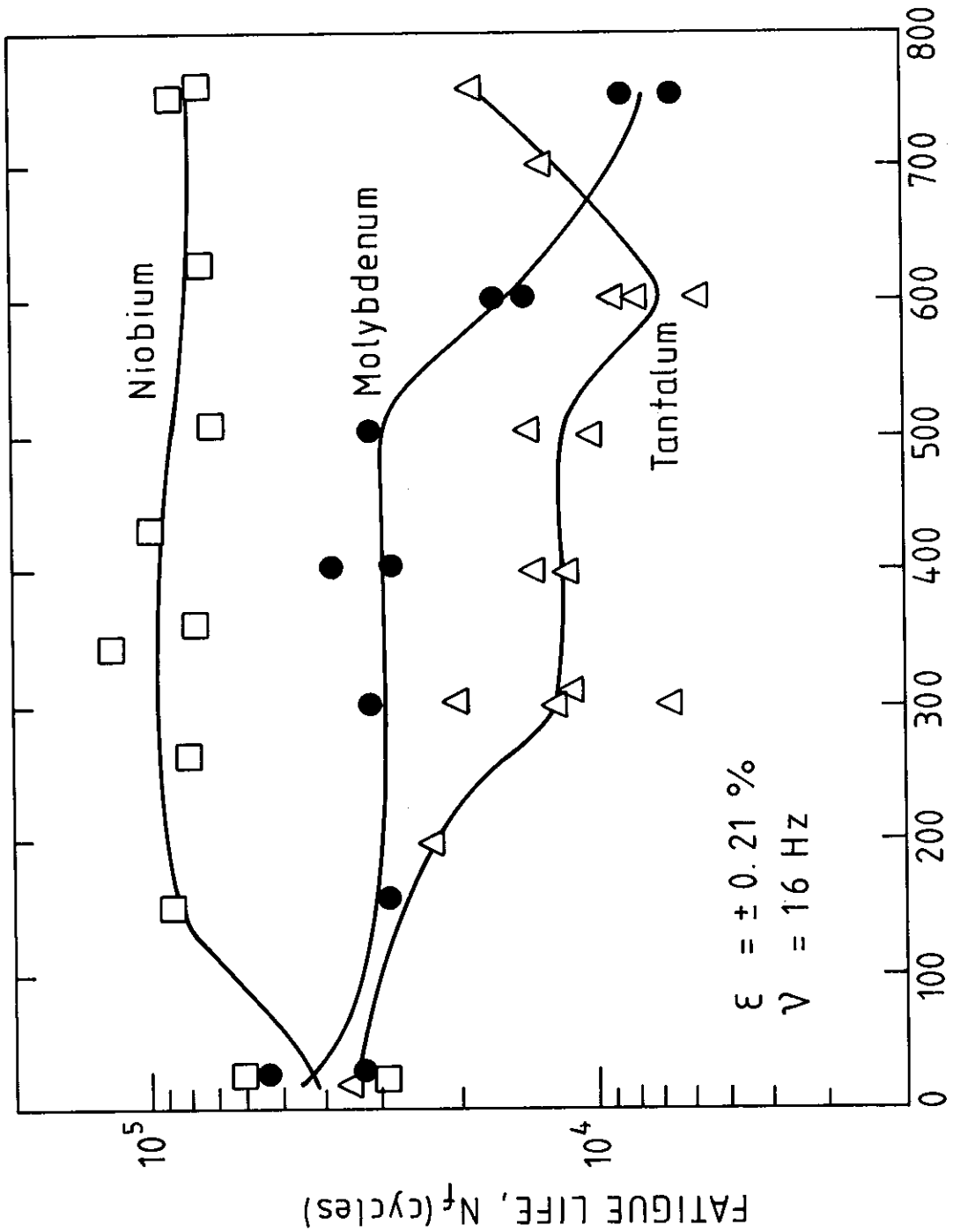

FIGURE 4. TEMPERATURE DEPENDENCE OF FATIGUE LIFE FOR NIOBIUM, TANTALUM AND MOLYBDENUM

A few two-stage tests were done on tantalum in which the specimen was first pre-fatigued at 400 or 750°C; the temperature was then raised or lowered to 750 or 400°C, respectively, and tested to failure. The results are as follows:

At 400°C

Pre-fatiguing at 750°C (N/Nf = 0.5) lowered Nf at 400°C by 53.6 per cent

Pre-fatiguing at 750°C (N/Nf = 0.25) lowered Nf at 400°C by 89.25 per cent

At 750°C

Pre-fatiguing at 400°C (N/Nf = 0.5) raised Nf at 750°C by 79.45 per cent

Pre-fatiguing at 400°C (N/Nf = 0.25) raised Nf at 750°C by 118 per cent

where N is the number of cycles and Nf is the number of cycles to failure.

The following points are noteworthy:

- Pre-fatiguing at 400°C followed by testing at 750°C increases the life at 750°C.
- Pre-fatiguing at 750°C followed by testing at 400°C decreases the life at 400°C.
- In both cases, the smaller the ratio N/Nf, the bigger is the effect on the fatigue life.

2.4 Effects of Pre-ageing and Prior Fatigue on Creep Behaviour

An investigation was made of the influences of prior ageing (at 750°C) and prior elevated-temperature fatigue (at 750°C) on the creep behaviour of type 321 stainless steel stressed at 200 MPa at 650°C. The prior treatments increased the creep rate and the ductility, and decreased the time to failure. The acceleration in the creep rate was proportional to $\varepsilon^{1.8}\, t_F^{0.68}$, where ε is the fatigue strain amplitude and t_F is the duration of the fatigue test and, in the case of pre-ageing, proportional to $t_A^{0.61}$, where t_A is the duration of ageing. Electron microscopy showed that, in the case of pre-ageing, the increased creep rate was associated with the growth of precipitates at triple

(a)

(b)

FIGURE 5(a): SUBGRAINS AND DISLOCATIONS AFTER 6 x 10^5 CYCLES AT A STRAIN AMPLITUDE OF ± 0.11% AT 750°C. (The arrow indicates where grain boundary migration has taken place.) (X 13 500)

(b): SUBGRAINS AND DISLOCATIONS AFTER SEQUENTIAL FATIGUE AT 750°C AND CREEP AT 650°C. (X 5 000)

junctions, along grain boundaries and within grains; however, sub-grain formation was not observed. Observations also revealed that in addition to the precipitation effects, the dislocation structures produced by prior fatigue persisted throughout the subsequent creep test. For example, after prior fatigue at 750°C, equi-axed sub-grains were formed. This was again evident after sequential creep at 650°C although the sub-grains were elongated rather than equi-axed (Figure 5). A stress-aided recovery mechanism may be responsible for these effects.

2.5 Development of Yielding Fracture Mechanics

Yielding fracture mechanics extends the aims of linear elastic fracture mechanics, namely, a quantitative assessment of the sensitivity of structures to defects and cracks, into the plastic region. It is used to enable assessment of the sensitivity of structures made of relatively ductile (more realistic) materials to cracks after widespread material yielding and some ductile crack growth.

(i) J_{1c} measurement

A PDP11/23 computer and two digital voltmeters have been purchased. Programming the computer to enable J_{1c} testing, using the single specimen compliance technique, is in progress. Measurements of J_{1c} have been made on a locally produced experimental C-Mn pressure vessel steel (BHP AB3501), using the multi-specimen technique.

(ii) Short rod testing

Grips have been manufactured to enable short rod testing. Material (MAR-300) has been received from ASTM and specimens are being machined as a contribution to an ASTM round-robin exercise to assess the short rod techniques for K_{1c} determination.

(iii) K_{1c} testing

The K_{1c} testing of Charpy size maraging steel specimens is complete. The tests show that there is a marked effect of holding time on the fracture toughness of MAR-350 at 900°C. The results were reported at the Melbourne Fracture Conference in August 1982.

3. SYNROC RESEARCH AND DEVELOPMENT

(Leader: K.D. Reeve)

3.1 Introduction

SYNROC is a synthetic three-phase titanate ceramic designed on the basis of known geochemistry for the immobilisation of high level nuclear waste at a 10 to 20 weight per cent level of addition. Collectively, the three SYNROC phases - barium hollandite ($BaAl_2Ti_6O_{16}$), perovskite ($CaTiO_3$) and zirconolite ($CaZrTi_2O_7$) - can take into solid solution almost all of the components of high level waste, and those which do not go into solid solution (for example, Mo, Tc, Ru, Pd, etc.) become micro-encapsulated as small particles of metal phase in the ceramic matrix. SYNROC, with or without non-radioactive simulated radwaste, may be synthesised from the component oxide powders, or from their nitrates or other precursors, and readily densified using well-known ceramic fabrication techniques.

Research and development on SYNROC commenced at Lucas Heights in March 1979, in association with a complementary program at the Australian National University. The Lucas Heights project consists of five main strands, namely:

(i) SYNROC Fabrication Development, using simulated radioactive waste but taking into account the difficulties inherent in the eventual use of high level waste.

(ii) Leach Testing of SYNROC, involving systematic atmospheric and hydrothermal tests.

(iii) Accelerated Radiation Damage Testing of SYNROC, using fast neutron irradiation to simulate actinide decay damage.

(iv) Supporting Research, including SYNROC mineral formation and fabrication studies and measurement of relevant mechanical and thermophysical properties of SYNROC.

(v) Heat Transfer Aspects of Underground High Level Waste Disposal, initially involving collection and evaluation of relevant heat transfer codes.

The project is inter-divisional, most of strands (i) and all of strands (iii) and (iv) being centred on Materials Division, strand (ii) and part of strand

(i) on Environmental Science Division, and strand (v) on Nuclear Technology Division.

3.2 SYNROC Fabrication Development

3.2.1 Laboratory process

The standard laboratory process for SYNROC fabrication starts with a ball-milled mixture of fine powders of TiO_2, ZrO_2, Al_2O_3, $CaCO_3$ and $BaCO_3$; to this is added sufficient nitrate solution of nine non-radioactive isotopes of high level waste (HLW) elements to achieve 10 to 20 wt % HLW oxides (see Table 2). The resultant slurry is spray- or flash-dried and then calcined in a stream of dry argon-3.5% hydrogen for 1 h at 750-800°C. The calcine is hot-pressed for 1 h in graphite dies at a pressure of 7-10 MPa and a temperature of 1150-1250°C. Densities of 98-99 per cent of the theoretical value are readily achieved.

TABLE 2
TYPICAL SYNROC COMPOSITIONS

SYNROC B		SYNROC C	
Component	(wt %)	Component	(wt %)
TiO_2	59.5	SYNROC B	85
ZrO_2	11.4	Simulated radwaste	10
Al_2O_3	6.0	Additional TiO_2	5
BaO[a]	7.2		
CaO[a]	15.9		
Simulated Radwaste			
CeO_2	9.7	ZrO_2	14.3
Nd_2O_3	28.3	Cs_2O	8.4
Eu_2O_3	4.4	SrO	6.2
FeO	9.6	NiO	2.8
MoO_2	16.3		
			100.0

[a] Added as carbonates

Routine characterisation tests on SYNROC C specimens cut from as-fabricated blocks include bulk density (normally close to 99 per cent of the theoretical value); open porosity (normally below 0.1 per cent); the presence of the three desired phases (by X-ray diffraction); and a check on the location of critical radwaste elements (by scanning electron microscopy with EDX analysis). In a complementary program funded by NERDDC and closely coordinated with that at Lucas Heights, the School of Science at Griffith University has begun to use a range of sophisticated techniques (including transmission and scanning electron microscopy, Auger spectroscopy, ESCA and SIMS) for more detailed characterisation of the crystalline and chemical structures of SYNROC before and after leaching.

3.2.2 Flowsheet development

The award in 1981-2 of a further NERDDC grant of $30 360 for SYNROC fabrication development (making a total grant of $244 426) has allowed the emphasis on the development of a realistic large-scale fabrication process to increase. From experience gained up to February 1982, the simplified fabrication flowsheet shown in Figure 6 was devised as a focus for further work. This has been mainly on the three key stages, namely SYNROC powder preparation (see Sections 3.2.3 and 3.2.4), calcination (see Sections 3.2.5, 3.2.6 and 3.2.7) and final consolidation (see Sections 3.2.8 and 3.2.9). As experience has been gained on these stages, the basic flowsheet has been progressively refined and plant layout constraints have been taken into account. The objective is to freeze the flowsheet by the end of 1982 (see also Section 3.2.10).

3.2.3 'Sandia' process studies

The standard laboratory process for SYNROC fabrication starts from oxide and carbonate powders and usually requires a hot pressing temperature of at least 1200°C. An alternative method of preparing SYNROC powder was demonstrated at Sandia National Laboratory* and is being studied and developed at Lucas Heights. The potential advantages of the 'Sandia' process are overall simplicity, improved chemical homogeneity and a reduction of the fabrication temperature - possibly by 50°C.

The process involves the hydrolysis of alkaline methanolic solutions of titanium tetra-isopropoxide and zirconium tetra-n-butoxide in acetone/water media to yield a sodium titanate/sodium zirconate powder mixture. This powder

* Dosch, R.G. and Lynch, A.W. [1980]. - SAND 80-2375.

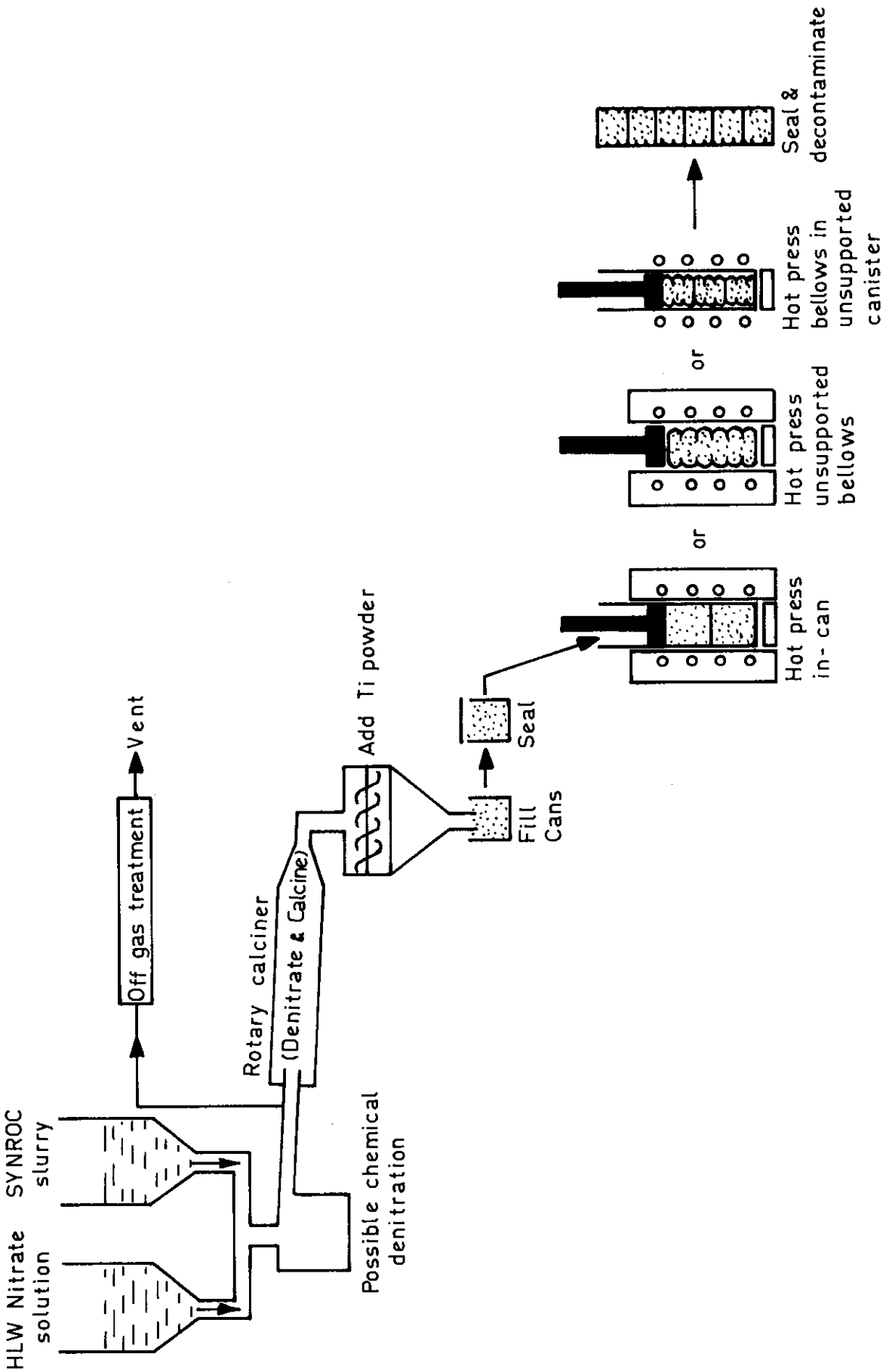

FIGURE 6. CONCEPTUAL FLOWSHEET FOR LARGE SCALE SYNROC FABRICATION

then acts as an ion-exchanger for an aluminium, barium and calcium nitrate solution to produce SYNROC B powder which has a high surface area and a high adsorptive capacity for radwaste ions from nitrate solution to form SYNROC C. The main aspects of the Lucas Heights work are as follows:

(i) Preparation, fabrication and leach testing of small batches of non-radioactive SYNROC C, using the process originally specified by Sandia. No difficulties were encountered. SYNROC densified to 97.4 per cent of theoretical density in 3 h at 1100°C and 13.8 MPa, whereas oxide-route SYNROC reaches only 91.7 per cent of theoretical under the same conditions. Sandia SYNROC has excellent leach resistance.

(ii) Studies on the effect of process variables on the surface area of Sandia-route SYNROC B powder. These showed that the surface area is relatively insensitive to the ratio of acetone to water used for hydrolysis of the alkoxides but is very sensitive to calcination temperature, decreasing rapidly between 600 and 1100°C. However, at 750°C, which is believed to be sufficiently high for a larger-scale process, the surface area of 16 $m^2\ g^{-1}$ was still excellent, compared with only 3 $m^2\ g^{-1}$ for oxide-route powder.

(iii) Study of the exchange of Na^+ in sodium titanate/sodium zirconate for Al^{3+}, Ca^{2+} and Ba^{2+}. This showed very rapid uptake of Ba^{2+} and slower, but still quantitative, uptake of Al^{3+} and Ca^{2+}.

(iv) Modification of the process towards simplification and lower material costs. Possible improvements being studied are reduction of the amount of acetone and avoidance of vacuum drying.

3.2.4 Large-scale powder preparation

As the scale of fabrication development work increased, the quantity of SYNROC powder needed for hot-pressing trials also increased. To conserve on-site technical effort, Alpha Chemicals (Aust.) Pty Ltd, of Dee Why, was commissioned to provide the following requirements:

(i) A 100 kg batch of Sandia-route SYNROC B powder to a detailed specification supplied by the Division as a result of laboratory experience with the Sandia process (Section 3.2.3).

(ii) Several batches of oxide-route SYNROC B powder totalling 400 kg, manufactured by a conventional slurry mixing/drying route proposed by the company.

In each case, the resultant powder was very similar to that prepared on a smaller scale at Lucas Heights and is being used very successfully in process and equipment development work.

3.2.5 Drying and calcination of SYNROC powder

All methods for making SYNROC involve the intimate mixing of solid SYNROC precursors with high level liquid waste. The mixture must then be dried and calcined to remove nitrates. There are a number of equipment choices for the drying/calcination stage including a spray calciner, a fluidised bed or a rotary calciner. Since the contact time in a spray calciner is short, complete denitration does not occur and a further calcination stage is required; this makes spray calcination unattractive for the SYNROC process. Drying and calcination can be effectively carried out in a single stage, using either a fluidised bed or a rotary calciner; both approaches are being examined.

3.2.6 Fluidised bed calcination

An existing 100 mm diameter fluidised bed was modified to study the drying/calcination of SYNROC powder. The initial charge to the bed was 5 kg of SYNROC B that had been crushed to $\sim$ 300 µm. A slurry comprising titanium and zirconium oxides in an acidified solution of aluminium, barium and calcium nitrates was sprayed onto the hot bed (450 to 600°C) through a pneumatic nozzle. In some experiments, waste elements (caesium, strontium and ruthenium) were added as nitrate solutions. The fluidising air was supplied at a constant rate of $\sim$ 2.5 $m^3\ h^{-1}$ while the slurry feed rate was varied from 1.5 to 7 $L\ h^{-1}$. The off-gas was passed through porous metal filters and scrubbed with a weak acid solution in a venturi scrubber followed by caustic potash solution in a packed column.

Two operational problems were encountered. In the initial experiments, blockage of the spray nozzle was a common occurrence. This was overcome by fitting a larger nozzle and reducing the heating directly adjacent to it. At high slurry feed rates, agglomeration that eventually led to loss of fluidisation occurred on several occasions. This arose when the heat input to the bed was momentarily insufficient for instantaneously drying the slurry. The bed became wet, resulting in local 'balling' of the powder, leading to

poor mixing in the bed, further agglomeration, cementation, and finally loss of fluidisation. Onset of this phenomenon could not be anticipated but it could be prevented by limiting the slurry feed rate to 4.5 L h^{-1}.

Apart from the above problems, the equipment operated satisfactorily with no significant increase in pressure drop across the filters and no problems in scrubbing nitrogen oxides from the off-gas. About 15 kg of SYNROC powder was produced at rates varying from 0.1 to 0.5 kg h^{-1}. The final bed contained less than two per cent of the original charge. The particle size of the powder increased during operation, about 10 wt % having a diameter greater than 1 mm. No significant build-up of small particles from attrition processes was observed, and the particle size distribution below 1 mm did not change significantly. Examination under the optical microscope indicated progressive 'spheroidising' of the < 1 mm fraction whereas the > 1 mm fraction contained a mixture of spherical particles and agglomerates. The agglomerates appear to be weaker than the spherical particles and are readily broken by light grinding.

Eight experiments were carried out to determine the extent of ruthenium volatilisation. Feed slurry spiked with ^{103}Ru was sprayed into the fluidised bed. Variables studied were acid concentration (0.25 and 4 M HNO_3) and fluidising gas (air or N_2/3% H_2). As was expected, the most oxidising conditions (air and 4 M HNO_3) resulted in the largest Ru volatilisation (4.0 per cent), whereas the most reducing conditions (N_2/3% H_2 and 0.25 M HNO_3) resulted in the smallest Ru loss (< 0.3 per cent).

The fluidised bed feasibility study is now complete. It showed that free-flowing, near-spherical particles can be produced with high pour (1.42 g cm^{-3}) and tap densities (1.57 g cm^{-3}). No major operational difficulties were encountered and, on a larger scale, even fewer problems are anticipated. A report describing the study is in preparation and will include an engineering assessment of the process for a full-scale plant.

3.2.7 Rotary calcination

Rotary calcination is considered to have several advantages over fluidised bed calcination: the gas volume requirement is smaller; bed blockage would be less likely to occur, and even if it did, it would be of little consequence. Rotary calcination has been used successfully for flash drying and partial denitration of radwaste nitrate solution in the French AVM high level waste vitrification process. To develop and assess this process

for SYNROC powder preparation on a reasonable scale, a rotary calciner was designed and built at Lucas Heights. The calciner is an inclined, slowly rotating stainless steel (Sandvik 253 MA) tube, 100 mm diameter by 1800 mm long. The tube is heated by a 50 kW (3 MHz) induction coil which also forms part of the in-can hot pressing system (see Section 3.2.8). The furnace is designed for a maximum temperature of 1000°C and allows a controlled reducing atmosphere (in the reference process, Ar-3.5% H_2) to be passed over the powder in the direction of powder flow.

Initially, the furnace was intended to re-calcine powder calcined in the fluidised bed. However, once the advantage of combining drying and calcination in one step became obvious, more attention was given to the concept of flash drying/rotary calcination. This was first shown to produce excellent SYNROC C powder using a mock-up laboratory process. The large rotary furnace was then modified for slurry injection by the provision of a water-cooled feed nozzle protruding into the hot zone. The first trials of the modified furnace with SYNROC B slurry containing no nitrates were very successful; trials with SYNROC/simulated radwaste nitrate slurry are about to commence. These trials will be at 750-800°C, which is now considered to be a adequate temperature range for the SYNROC process.

3.2.8 In-can hot pressing

(i) Description

The in-can hot press (Figure 7) consists of a specially designed induction furnace, in which closed-end stainless steel tubes (115 mm o.d.) are provided with lateral support and loaded progressively with SYNROC powder or granules, together with a 50 tonne hydraulic pressing (top) ram and a 15 tonne ejection (bottom) ram.

The induction coil consists of seven segments. Power from the 50 kW (3 MHz) induction coil can be switched between segments almost instantaneously at full power. Each segment is provided with a refractory sighting tube which, in conjunction with an infrared sensing head, allows direct measurement and control of the surface temperature of the stainless steel. The sensing head is manoeuvred by hand into the viewing position of each refractory tube in turn, a change from one zone to the next taking only about five seconds. The SYNROC powder is heated by heat transfer from the stainless steel susceptor/canister/die.

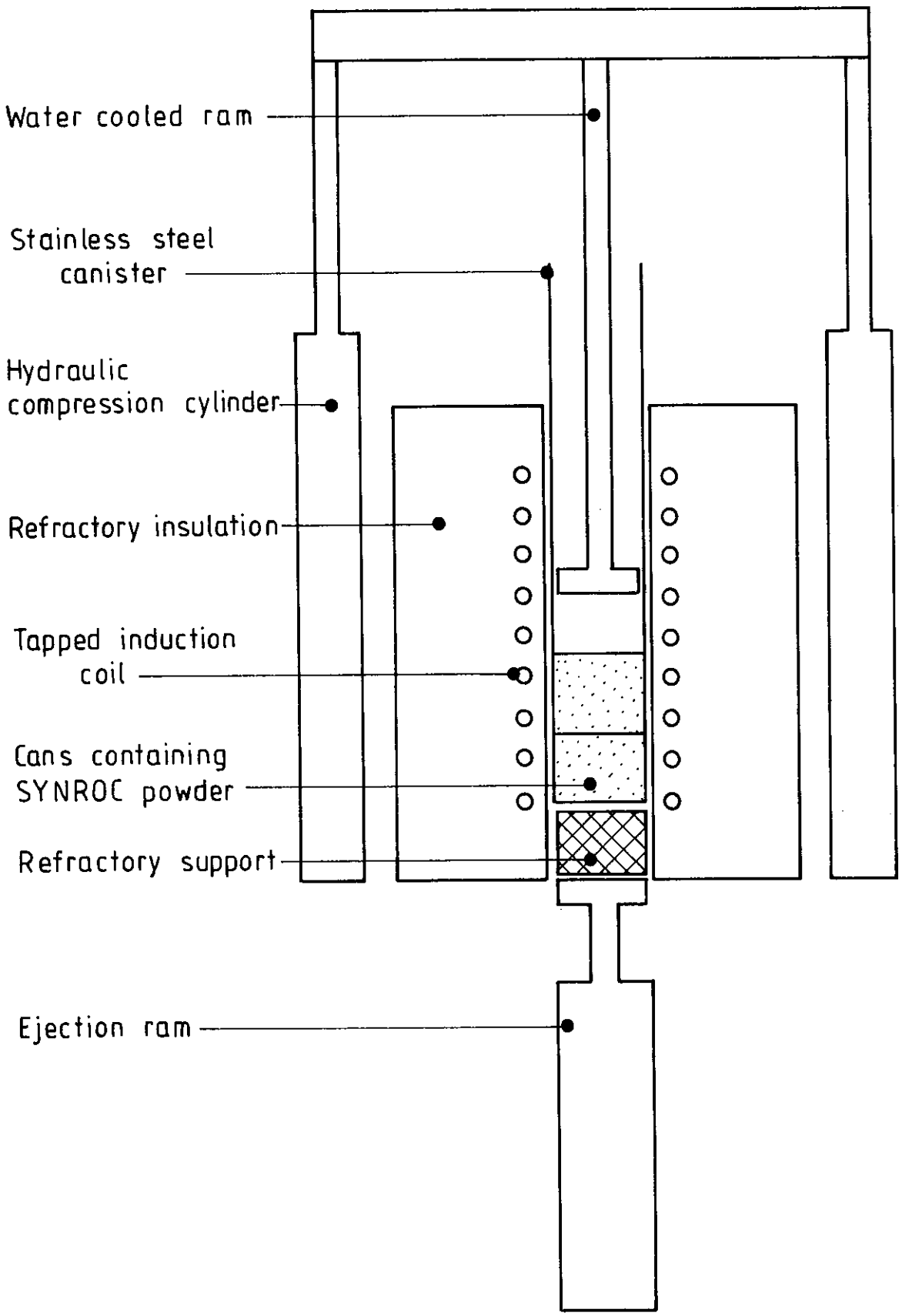

FIGURE 7. SCHEMATIC CROSS-SECTION OF THE IN-CAN HOT PRESS

The pressing ram consists of a water-cooled shaft fitted with a replaceable pressure pad and linked to two precisely aligned hydraulic cylinders. The location of the pad face is continuously monitored and the pressing ram is retracted hydraulically by the operator when the pad is 60 mm above the hot zone.

The recirculating water cooling system incorporates two separate pumps, and an emergency gravity-fed tank supply operates automatically in the event of power failure.

(ii) Powder preparation for in-can hot pressing trials

The in-can hot press was commissioned with SYNROC B powder, but trials with simulated radwaste-doped SYNROC C have not commenced. The SYNROC B was made as follows. Powders of TiO_2, Al_2O_3, $BaCO_3$, $CaCO_3$ and ZrO_2 were wet-milled with zirconia media in small batches in an attritor for 20 minutes. The creamy aqueous slurry was air-dried in trays at 120°C and the dried cake calcined in 15 kg batches in refractory containers in air at 950°C for 16 h. The calcined powder was then micronised. Calcined/micronised powder batches were blended to produce two 100 kg batches which were sealed in polythene bags to await use.

The tap density of the powder was 0.86 g cm^{-3}. X-ray diffraction showed that all three expected SYNROC phases (barium hollandite, perovskite and zirconolite) had started to form, although precursor oxide patterns were also present. Small graphite die pressings made from this powder densified to 4.22 g cm^{-3} (99 per cent theoretical) in 3 h at 1250°C and 10 MPa.

(iii) Operating experience with the in-can hot press

For each trial pressing, approximately 31 kg of SYNROC B powder was loaded into 26 mild steel cans on a simple vibrating table to a packing density of 1.2 g cm^{-3} (approximately 28 per cent theoretical). Each can (98.5 mm diameter x 152 mm high x 0.24 mm wall thickness) was sealed with a press-fitting lid. This procedure simplified powder loading to the press, minimised dust formation during the process and prevented the extrusion of SYNROC upwards between the ram and the canister wall during hot pressing.

The canister was prepared from Sandvik 253MA stainless steel tubing (115 mm o.d. x 100 mm i.d.). A 2 m length of tubing was closed at one end with a

welded 7.5 mm end-cap, then positioned vertically in the press with the lower 1 m of tube in the heated length of the furnace; it was then preheated in air at 1250°C for 30 minutes to form a protective Cr_2O_3 surface film.

Four cans, each containing 1.2 kg of SYNROC powder, were loaded into the canister. Full power was then applied to the first (bottom) zone. The canister wall reached the chosen control temperature of 1230°C in approximately four minutes, whereupon a load of 9 tonnes was applied to the four cans with the main compression ram. This pressure (9.9 MPa) was maintained automatically by the hydraulic control system throughout the whole pressing operation, except when the ram had to be raised to add more cans of SYNROC.

Plastic flow commenced in the SYNROC after 20 minutes' heating, and 90 per cent densification was reached after 90 minutes. When the pressure pad was 60 mm above the hot zone, the compression ram was withdrawn and moved sideways hydraulically to allow two more cans of SYNROC to be added. This procedure took 5-7 minutes, full power heating being maintained throughout. Pressing was continued for a further 90 minutes, after which it became apparent that no further densification was occurring. Power was then switched to the second zone, two more cans of SYNROC were added and a similar sequence of operations followed. In successive zones, the number of cans varied between three and four to make 26 in all. In the seventh and last zone, a 60 mm thick refractory spacer was inserted above the top can so that when complete densification was achieved the face of the pressure pad would still be 60 mm above the hot zone.

The heating/pressing operation for the seven zones took 21 hours. The hot-pressed canister was allowed to cool <u>in situ</u> for six hours before being ejected vertically upwards via the bottom ram. The length of the canister above the ceramic spacer was then cut off and a stainless steel top end-cap welded on.

(iv) <u>Results</u>

Five canisters of SYNROC B were produced. Surface oxidation and scaling were minimal. The average increase in diameter was 2 per cent, with a very small variation (± 1 per cent) except at the seven sighting-tube positions, where there was a local increase of up to 5 per cent in the overall diameter. Several 10 mm diameter cores were trepanned from the canister at various

positions and the corresponding density of the SYNROC was measured. Values of 97 to 99 per cent theoretical density were obtained. X-ray diffraction on the same cores showed that the three expected SYNROC minerals were well-formed. Windows for visual inspection were milled in four positions along one side of each of four canisters. These showed that the inner cans had shortened by forming shallow folds near the inner surface of the canister. This behaviour was not unexpected and was not considered in any way detrimental to either the SYNROC or the canister.

Previous laboratory experience suggests that SYNROC C will hot press slightly more easily (e.g. at temperatures up to 50°C lower) but otherwise will produce very similar results.

The demonstration of in-can hot pressing for the fabrication of 30 kg canisters of SYNROC is a major milestone in the development of this advanced high level waste form. An Australian concept named by analogy with the 'in-can glass melting', this process has no intrinsic features which would prevent its further scale-up and application to the incorporation of actual high level waste. Those aspects of the present demonstration rig which require manual operation, e.g. loading of SYNROC cans and re-positioning of the control pyrometer for each zone, could certainly be simplified and automated for remote operation. Another aspect requiring attention is the relatively long cycle time; experiments have commenced on the present rig with the aim of reducing this problem. Further improvements are possible by systematically pre-heating the SYNROC immediately above the hot zone and by using more sinterable SYNROC powder to reduce the time required for densification. A 100 kg batch of Sandia-route SYNROC, which has a higher surface area and is significantly more sinterable, has been prepared and will be in-can hot pressed as SYNROC C in the near future. Tests on the product will include the measurement of caesium, strontium and europium leach rates on samples machined from drilled cores.

3.2.9 Bellows hot pressing

During the construction of the in-can hot press, another uniaxial hot pressing method was conceived which could be attractive for scale-up and commercial operation, namely the hot pressing of SYNROC in unsupported thin-walled bellows. This and a hybrid concept - the use of bellows-type cans within a canister which would need no support during hot pressing - are being assessed against the original in-can hot pressing concept. Unsupported bellows, up to 30 cm diameter and containing 25 kg of SYNROC B, have been

successfully hot-pressed but further work is necessary to define the optimum bellows design and pressing conditions. A small rig has been built on which to test the alternative 'in-can bellows' process on a 10 cm diameter scale, using the same thick-walled outer stainless steel tubing as for the original in-can hot pressing development.

3.2.10 Proposed SYNROC fabrication pilot plant

In March 1982, the AAEC submitted a new policy proposal to the Australian Government to allow a fully engineered, non-radioactive fabrication pilot plant able to demonstrate all stages of the fabrication of full-scale SYNROC canisters to be built at Lucas Heights. Although no decision on this proposal has been announced (as at 30 June), the SYNROC fabrication program is proceeding on the assumption that a choice must be made between in-can hot pressing and one of the two bellows hot pressing concepts by the end of 1982.

3.2.11 Comparison of costs for glass and SYNROC

Tentative cost estimates were made for solidifying and disposing of high level liquid wastes in SYNROC and borosilicate glass. In each case, the solidification plant was designed to accept wastes from a reprocessing plant with a throughput of 2000 t U/year. This scale of operation enabled cost data and cell layouts to be taken from the US Final Environmental Impact Statement on Management of Commercially Generated Radioactive Waste (DOE/EIS-0046F). The waste canisters were assumed to be 0.3 m diameter x 3 m high with a calcine loading of 20 wt % for SYNROC and 10 wt % for glass. In keeping with European practice, the 10 wt % waste loading in glass was chosen because of the need to limit glass surface temperature so as to avoid excessively high leach rates.

A number of processing alternatives were considered for SYNROC fabrication including oxide versus Sandia routes, and hot uniaxial pressing in cylinders or bellows versus hot isostatic pressing. The Sandia route increased unit costs for solidification by about 30 per cent but the various hot pressing options had little effect.

The major cost disadvantage of glass was the need for interim storage to allow the glass to cool below 100°C. Overall, the cost estimates showed a significant overall cost saving for SYNROC compared to glass. However, to validate this conclusion it will be necessary to demonstrate the design concepts for SYNROC on a full scale.

3.2.12 Radioactive SYNROC fabrication

In March 1982, a NERDDC grant of $230 000 was awarded to allow the construction and operation of two lines in which low levels of radioactive waste elements can be added to SYNROC and leach test specimens produced by hot-pressing:

(i) An actinide line, in which ^{237}Np, ^{239}Pu, ^{241}Am and ^{244}Cm will be added separately to produce leach test discs each containing approximately 100 μCi (3.7 MBq) of the relevant actinide.

(ii) A hot cell line, in which fission product waste from the Lucas Heights technetium generator project can be added to SYNROC to produce leach test discs and at the same time immobilise the site waste that is now stored as an acid solution. The total activity of the fission product waste is approximately 300 Ci (10 TBq); however, this will not be useable in the SYNROC project until most of the residual uranium has been extracted and the solution concentrated. This is to be done by Dr J.M. Costello of Environmental Science Division as part of the 'Waste Treatment and Disposal' project.

Detailed planning for the two radioactive SYNROC lines has commenced and some of the equipment is about to be ordered, with the objective of commissioning both lines early in 1983.

3.3 Leach Testing of SYNROC

About 500 leach tests were carried out for routine evaluation of developmental SYNROC specimens and for systematic comparison of the leach resistance of SYNROC and borosilicate glass. A number of general conclusions can be drawn from these tests:

- SYNROC C is more leach resistant than borosilicate glasses over the temperature range 45 to 300°C.

- The leach rate of SYNROC does not increase greatly with temperature. As temperature is increased from 100 to 300°C, the leach rate of SYNROC increases by a factor of about eight whereas that of borosilicate glass increases by a factor of about fifty.

- The leach rate of SYNROC decreases rapidly with time.
- The matrix elements in SYNROC, particularly Ti, Zr and Al, are very resistant to leaching.
- Caesium is the most leachable radwaste element in SYNROC.
- Leach rates of SYNROC in deionised water and brine are similar.

The leachability of SYNROC has been measured using a number of standard procedures, including the ISO/IAEA long-term leach test, and static (MCC-1) and dynamic (MCC-4) tests developed by the Materials Characterization Center (MCC) at Batelle Pacific Northwest Laboratories (PNL), Hanford, USA. These tests simulate the extreme environments likely to occur in a waste repository, ranging from totally static conditions to those where the groundwater surrounding the waste is rapidly replaced. The ISO test procedures have been modified to the extent that the leachant is replaced daily rather than with the decreasing frequency recommended in the test. Monolithic specimens were leached wherever possible, but in some cases powders were used because the leach rates of monolithic specimens were below the limits of detection. Provided that geometric rather than BET surface areas are used, leach rates for monolithic and powdered SYNROC are in reasonable agreement.

Figure 8 compares the leach rates of Cs and Sr from SYNROC C and borosilicate glass (PNL 76-68). Under modified IAEA/ISO test conditions at 100°C, the glass leaches congruently at a rate of 2 g m^{-2} day^{-1}. In contrast, the leach rate of Cs and Sr from SYNROC decreases with time and, after 70 days, is 1/1000th that of glass. The leach rate of Cs is initially much higher than Sr but, after 30 days, the leach rates of both elements are similar.

Figure 9 shows the results of MCC-1 tests carried out in demineralised water at 90°C using SYNROC and borosilicate glass (PNL 76-68). The normalised 30-day average leach rates (g m^{-2} day^{-1}) for SYNROC matrix elements were:

$$Ti = 1.1 \times 10^{-4} \quad Zr < 4 \times 10^{-4}$$
$$Al < 9.7 \times 10^{-3} \quad Ba = 1.5 \times 10^{-2}$$
$$Ca = 1.4 \times 10^{-2}$$

The equivalent leach rates for matrix elements from PNL 76-68 were Si = 0.73,

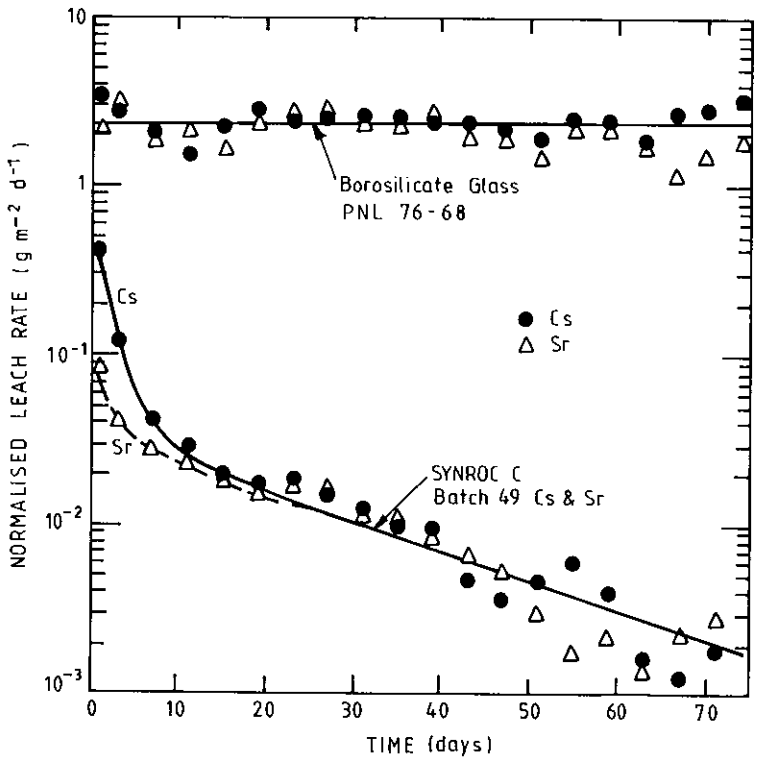

FIGURE 8. LEACH RESULTS FOR CAESIUM AND STRONTIUM FROM SYNROC C AND WASTE GLASS PNL 76-68 AT 1000°C (LEACHANT : DEIONISED WATER, REPLACED DAILY)

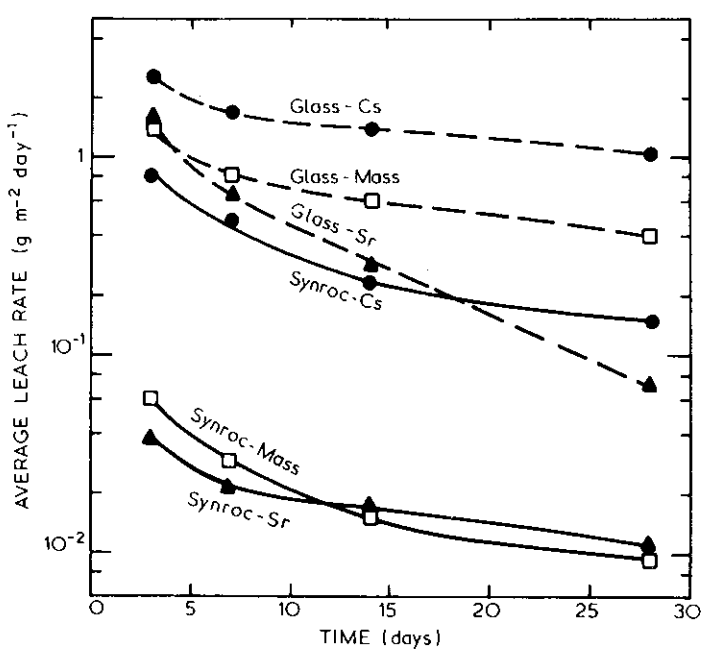

FIGURE 9. COMPARISON OF STATIC LEACH TESTS (MCC-1) ON SYNROC (BATCH 86) AND BOROSILICATE GLASS (PNL 76-68)

B = 1.12, and Ca = 6.8×10^{-2}. Under MCC-1 test conditions, SYNROC is clearly superior to borosilicate glass although not to the same extent as under ISO or dynamic leach conditions. The reason for this is that, under static conditions, the leach rate of glasses decreases as saturation of the solution is approached. In addition, strontium and most heavy metals are precipitated or adsorbed onto the siliceous layer at the high pH (>9) encountered in static leach tests.

Dynamic leach tests (MCC-4) were carried out on SYNROC at 90°C for 28 days. A peristaltic pump was used to meter demineralised water to the leaching vessel at a rate of 15 mL day^{-1}. The leach results were similar to those obtained in static leach tests (MCC-1) for the same period.

The data shown in Figures 8 and 9 are based on experiments in demineralised water using 10 wt % simulated radwaste in SYNROC produced via the oxide route. SYNROC prepared by the Sandia route exhibits lower leach rates for Cs and Ca but otherwise is similar to oxide-route material. At least 20 wt % radwaste can be incorporated in SYNROC without a significant increase in leach rate. It should be noted that, because SYNROC has a higher density than glass, a 20 wt % radwaste loading is equivalent, on a volume basis, to a 30 wt % loading in glass. The fact that SYNROC will accept this higher waste loading has important economic implications.

A systematic study has been made on the effect of fabrication conditions on the leach resistance of SYNROC. Table 3 lists the fabrication variables in their approximate order of importance. A reducing atmosphere during calcination is essential to prevent the formation of soluble caesium molybdate. Likewise, it is recommended that Ti powder be added immediately before hot pressing to control oxidation potential during fabrication. Initially, a calcination was carried out at 1100°C for 16 hours for complete mineralisation, but recent studies have shown that 800°C for one hour is sufficient to produce leach-resistant SYNROC. Use of these less stringent conditions in a processing plant will increase calciner throughput yet reduce losses of volatile radwaste elements. The density of leach-resistant SYNROC can be as low as 96 to 97 per cent theoretical, provided that there is no open porosity present. Thus the requirements and control needed to fabricate leach-resistant SYNROC are not unduly demanding.

TABLE 3
RELATIVE IMPORTANCE OF SYNROC FABRICATION CONDITIONS
ON LEACH RATES

Relative Importance	Fabrication Variable	Conditions Studied
Important	Redox control during calcination	Air, CO_2-7%CO, 3.5% H_2 in Ar*
Limited importance	Homogeneity of mixing	Mechanical blending, ball-milling, Sandia route*
	Hot pressing temperature	1100-12590°C (1200°C*)
	Redox control during hot pressing	Addition of Ni, Fe, Ti*
Non-critical for conditions studied	Waste loading	10-20* wt %
	Calcination temperature	800*-1100°C
	Calcination time	*1-17 hours

*Indicates favoured conditions

3.4 Radiation Damage Testing

3.4.1 Fast neutron irradiation

Fast neutron irradiation is being used to produce displacement damage in SYNROC B (without waste), SYNROC C (with 10 per cent simulated waste), barium hollandite, zirconolite and perovskite to simulate the actinide decay damage which will accumulate during long-term disposal of SYNROC with radwaste. The correlation of fast neutron and actinide decay damage is done by equating the calculated displacements per atom for the two cases, on the basis of 10 and 20 wt % addition. The macroscopic, microscopic and crystal structure effects are being measured on all five materials for SYNROC 'ages' up to 10^6 years, obtained by irradiating to a fast neutron dose of 4×10^{20} neutrons cm^{-2} (> 1 MeV). Materials variables include the fabrication method (cold pressing and sintering versus hot pressing) and the presence or absence of simulated radwaste.

Macroscopic and microscopic effects

All materials have increased in volume and correspondingly decreased in density with longer fast neutron exposure and simulated SYNROC age. For the same exposure, these effects increased in the order barium hollandite ≈ hot-pressed SYNROC B < perovskite ≈ zirconolite ≈ SYNROC C < cold-pressed and sintered SYNROC B. The reason for the marked effect of fabrication method on the expansion of SYNROC B (Figure 10) is being investigated. However, there is very little effect of fabrication method on the irradiation behaviour of SYNROC C. A tendency to saturation is evident at the longest irradiations, i.e. equivalent to 9×10^5 years on a 10 wt % basis.

Each of the SYNROC phases has an anisotropic crystal structure which expands differently upon irradiation. Build-up of grain boundary stresses leading to microcracking is therefore expected. Although all SYNROC specimens remained intact after irradiation and showed no sign of physical deterioration, metallographic examination has revealed microcracking for volume expansion levels above 4 per cent. No microcracking has been detected below this level. Microcracking is accompanied by only a small increase in the open porosity; for the greatest expansion recorded (8.6 vol. %), this increase amounted to only 0.03 per cent of specimen volume.

In SYNROC C, the microcracking level corresponds to a SYNROC age (on a 10 wt % basis) of 2×10^5 years (Figure 10). Preliminary leach tests at 40°C on SYNROC C, irradiated to simulated ages of 10^4 and 2×10^5 years, have shown no marked change in leach rate for caesium over unirradiated control specimens. Leach tests on more heavily irradiated specimens are planned but, as the increase in open porosity has been small, no increase in leach rate is anticipated.

X-ray diffraction studies

After barium hollandite has been irradiated to a dose of 6.5×10^{19} neutrons cm^{-2} (> 1 MeV), all high-angle X-ray reflections (> 70° 2θ) are eliminated and low-angle reflections are selectively broadened and attenuated. The lattice parameter changed by +0.10 per cent in the a-direction and -0.36 per cent in the c-direction, leading to a decrease in the unit cell volume of 0.16 per cent. These results have been interpreted in terms of the production of isolated stress centres and dislocation loops within the structure. A paper is being prepared for publication.

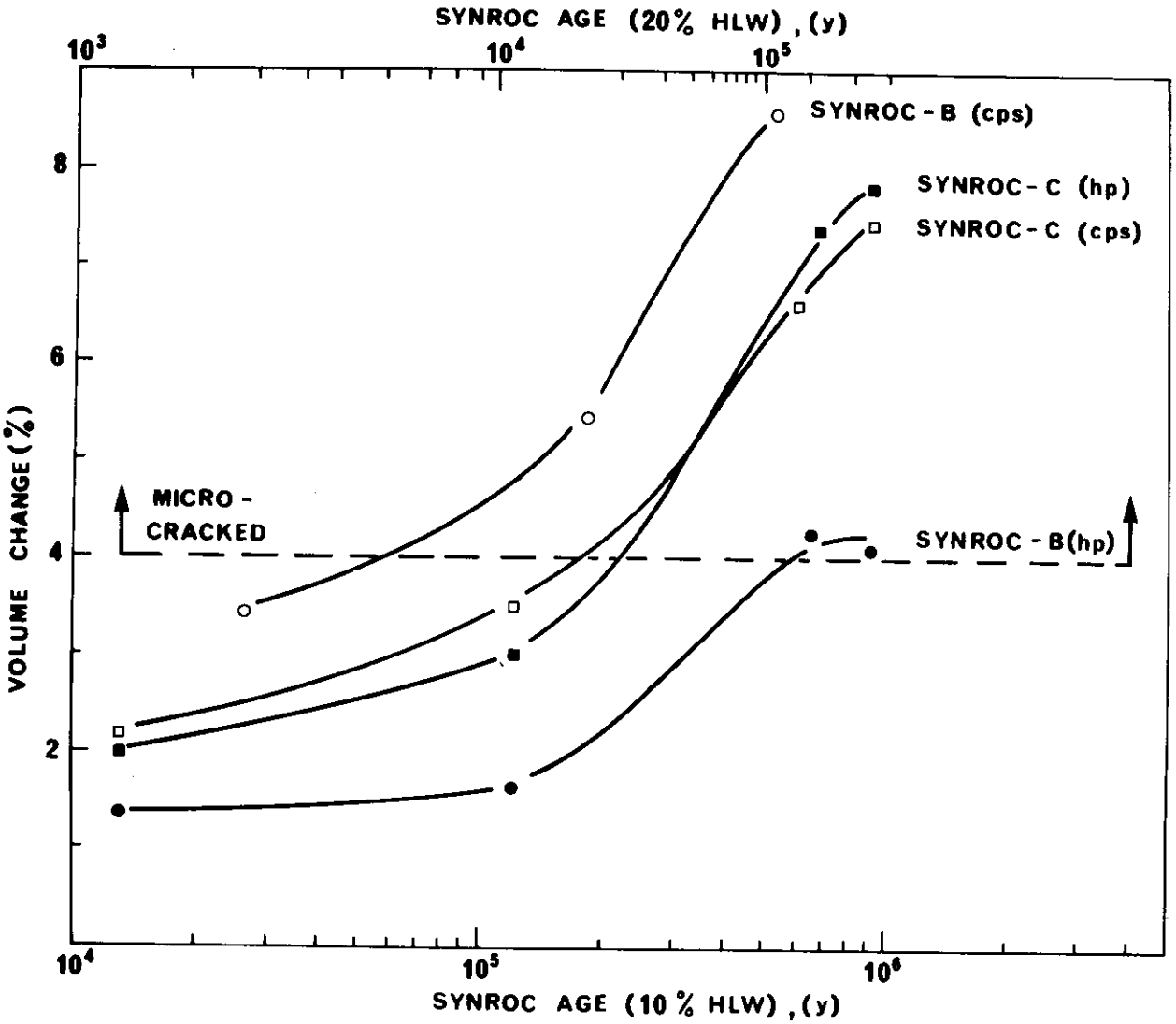

FIGURE 10. VOLUME EXPANSION OF FAST NEUTRON IRRADIATED SYNROC AS A FUNCTION OF 'SYNROC AGE' (cps = cold pressed and sintered; hp = hot pressed)

3.4.2 External alpha irradiation

In a collaborative program started in 1980, specimens of hollandite, perovskite and zirconolite made at Lucas Heights are being subjected to external alpha irradiation at PNL in parallel with fast neutron irradiation of similar specimens at Lucas Heights. Results have been received regularly from PNL as their alpha irradiation proceeds. However, the displacements per atom so far achieved at PNL - 0.050, 0.028. and 0.024 respectively - are still very low compared with those from neutron irradiation at Lucas Heights - 0.7, 0.7 and 1.0 respectively.

The PNL technique is probably most relevant for the hollandite which, in SYNROC containing actual radwaste, is subjected to α-particle damage only; in contrast, the perovskite and zirconolite are damaged mainly by α-recoil nuclei. The PNL results already cover a hollandite 'age' of about 10^5 years, whereas the Lucas Heights results start at $\sim 10^6$ years. For hollandite, it appears that neutron irradiation is underestimating the actual α-particle damage. This is because α-particles produce less of a thermal spike and are therefore less self-annealing. For perovskite and zirconolite, neutrons will be better than α-particles for simulating the dominant actinide recoil damage.

A joint PNL-AAEC paper on this collaborative project is foreshadowed for drafting towards the end of 1982.

3.4.3 Actinide doping of zirconolite

Zirconolite has been doped for radiation damage assessment with ^{244}Cm at PNL and ^{238}Pu at Los Alamos National Laboratory. These studies are complementary to the Lucas Heights neutron irradiation study on the same material, and results have been exchanged between the three laboratories. These results, correlated on a displacements per atom basis, are in surprisingly good agreement and an inter-laboratory research paper is foreshadowed.

3.5 Supporting Research

3.5.1 Thermophysical properties

The thermal diffusivity, specific heat and thermal conductivity of perovskite, hollandite, zirconolite, SYNROC B and SYNROC C, each made by hot pressing (HP) and cold pressing and sintering (CPS), have been measured against temperature using the laser flash technique. The results are shown in Table 4.

TABLE 4
THERMAL DIFFUSIVITY VALUES (x 10^6 m^2 s^{-1})

Material	CPS	HP		$\frac{\alpha_1-\alpha_2}{\alpha_2}$ (%)
		α_1	α_2	
Perovskite	1.595	1.653	1.619	2.1
Hollandite	1.11	1.298	1.229	5.6
Zirconolite	0.88	1.003	0.968	3.6
SYNROC B	1.07	1.212	1.138	6.5
SYNROC C	0.92	1.113	0.951	17.0

α_1 = α at right angles to HP direction
α_2 = α parallel to HP direction

The property values obtained for SYNROC and its mineral phases fall in the broad range for titanates and decrease in the order perovskite > hollandite > zirconolite. Values for SYNROC B are close to those for hollandite, whereas the values for SYNROC C are closer to those for zirconolite. The thermal diffusivity curves pass through a minimum at 400 to 500°C with a slight increase at 650°C. The specific heat increases with temperature. The thermal conductivity of perovskite decreases slightly with increasing temperature, whereas the other materials exhibit a slight increase.

Since all the constituent mineral phases of SYNROC have non-cubic crystal symmetry, their single crystals are expected to be anisotropic with respect to thermal conductivity. In CPS polycrystalline ceramics, the anisotropic crystals are randomly oriented and properties show no net directionality; however, preferred orientation can occur in HP and extruded ceramics and property values can be dependent on direction. Consequently, the thermal diffusivity of the HP materials was measured in two directions, with the heat flow parallel or at right angles to the hot pressing direction. Table 3 shows that the directional effect is small but real in the individual HP mineral phases. The directional effect in SYNROC B is perhaps slightly higher than expected for a mixture of these phases but, surprisingly, it is much higher in SYNROC C. Preliminary microscopy of polished sections indicated a minor phase of rod-shaped particles aligned at right angles to the hot pressing direction in SYNROC C; no alignment was evident in the other directions. This phase

was not found in SYNROC B nor in the individual minerals; its nature and the effects are being investigated.

3.5.2 Fatigue behaviour

In an informal collaborative program with Materials Division, Dr B.R. Lawn, formerly of the Department of Applied Physics at the University of New South Wales and now a member of Fracture and Deformation Division, National Bureau of Standards, is studying the dynamic fatigue response of SYNROC B and borosilicate glass specimens in water, using an indentation flaw technique. SYNROC appears to be intrinsically stronger than borosilicate glass but it has a similar susceptibility to fatigue. A joint paper on this work is in press.

3.6 Heat Transfer Aspects

A literature survey on high level waste disposal in underground repositories is in progress. Available heat transfer codes applicable to the calculation of space- and time-dependent temperatures for SYNROC disposal have been surveyed and the code HEATING 5 has been ordered.

4. METALLURGY AND ASSESSMENT

(Leader: R.J. Hilditch)

4.1 Non-destructive Testing

4.1.1 Neutron radiography

(R.J. Hilditch, N.W.D. Chrimes, P.A. Gillespie)

The routine radiography of door opening thrusters has continued. A preliminary examination has been made for Qantas of a jet engine component that had been repaired by brazing. Neutron radiography was feasible since the brazing alloy contained boron, a neutron absorbing material.

As an aid to research by AINSE fellows, neutron radiographic techniques have been used to monitor the root growth of soya beans. This work has been extended to an examination of the root growth of pinus radiata seedlings.

A contract with Aeronautical Research Laboratories for the neutron radiography of aluminium alloy samples to detect corrosion damage has continued.

4.2 Ultrasonics

(R.J. Hilditch, N.W.D. Chrimes, D.S. Bloser)

4.2.1 General development work

An ultrasonic phototechnique for imaging composite materials has been developed. Reflected ultrasound signals are used to modulate a flying light spot and the resulting amplitude variations produce scanning patterns which are recorded on Polaroid film.

An autoplot manual scanning system is being developed to enable manual scanning in any direction. The resulting data are plotted on a visual display unit in real time. Such data can be stored for analysis when required, and hard copy is also available from the printer.

An Apple II Plus computer has been interfaced to the ultrasonic test tank via a slave microprocessor to handle routine functions. This enables the computer to perform the analysis and image plotting quickly and efficiently.

Computer programs have been written for a number of applications:

- Isometric C scan projections
- Zoomplot spectral analysis
- A/D canister control program
- Synchronous signal processing and timing
- Data handling and control
- Three-dimensional image projection

4.2.2 Liaison with outside organisations

Work has been carried out for the following organisations:

BHP, Clayton, Victoria Detection of sulphides and oxides in rail steels using ultrasonic spectroscopy.

Hawker de Havilland, Bankstown, NSW Advice on the design and manufacture of a test tank for immersion testing, and associated electronics.

Omark Ltd, Lansdale, SA Development of test procedures for the examination of railway sleepers with electrically-resistant welded attachments.

Aeronautical Research Laboratories, Melbourne Investigation of the use of ultrasonic testing or examining corroded aluminium samples (this work is complementary to the ARL neutron radiography contract).

4.3 Metals Fabrication

4.3.1 Investigations related to commercial bulk analyser unit

(R.J. Hilditch, A. Ridal, B. Cooper)

Silica ampoule compatability tests

(a) With ZnI_2 Compatibility tests, carried out at 1000°C for 10 000 h, showed no visual difference between silica ampoules with and without ZnI_2. Absence of a reaction was confirmed by scanning electron microscopy but there was an increase in size which was attributable to the greater atmospheric pressure (12 atomospheres instead of 1).

(b) With $Co/Al/Br_2$ This compound was investigated because of problems encountered with the diffusion of cobalt in silica. Two ampoules containing $Co/Al/Br_2$ and one containing bromine were tested for 1600 h at 550°C and a pressure of $\sim$ 8 atmospheres; there was no dimensional or chemical change. The test is continuing up to 10 000 h.

Reported failure of Greenvale source

A bulk analyser source installed at Queensland Nickel Pty Ltd, Greenvale containing ^{60}Co iodide was reported to have failed after 1172 h at 860°C (reputedly 990°C as explained below) with cycling to ambient temperature on 108 occasions over 8 months. The stainless steel capsule showed no appreciable corrosion and the silica ampoule only a small surface cavity of indeterminate depth. No cracking or Co diffusion was noted although the inside surface was coated with crystalline CoI_2.

Thus the ampoule appeared to be satisfactory apart from a possible 'pin-hole' cavity which had not allowed all the CoI_2 to escape. The fact that no reaction had occurred on the inside of the silica suggests that the true operating temperature was in fact nearer 860°C than 990°C.

4.3.2 Investigations involving maraging steels

(R.J. Hilditch, A. Ridal, R. Hemphill)

Assessment of fabrication history

Three groups of cold-formed 350 grade maraging steels from CEPD were examined to determine the fabrication route and compliance with the specification. The results of chemical analysis, metallography, micro hardness and texture indicated that all specimens complied with the maker's specification for the amount of cold work carried out.

Effect of heat treatment on density of 350 grade maraging steels

Two materials, designated Sandvik 350 and German 350, were examined. After solution treatment for 1 h at 900°C and reheating at 50 degree steps in the range 200 to 400°C without resolution treatment, the maximum density changes were 1.4 per cent for Sandvik 350 at 700°C and 1.5 per cent for German 350 at 710°C.

4.3.3 Service work

(A. Ridal, S.E. Rowling, B.C. Cooper, F. Atkins)

The principal activities were as follows:

Melting and casting	6 uranium castings (EFCO furnace), 2 uranium castings (10 kg induction furnace); 2 iron titanium manganese alloys.
Fabrication (pressing/rolling)	Maraging steels, stainless steels, titanium alloys, platinum.
Heat treatment	Annealing, hardening, tempering.
Machining	SYNROC machining including exhibits for the World Fair held at Knoxville, USA. (This was approximately 90 per cent of the effort.) 28 miscellaneous jobs including uranium, maraging steels iron nickel alloys, alumina, porcelain, glass, beryllium oxide.
External services	5 kg of depleted uranium turnings for CSIRO. Depleted U mouthguard (Sydney Hospital). Uranium penetrators for Defence Standards Laboratory, Melbourne.

4.4 High Activity Handling Cells

4.4.1 No.1 block

(G. Mitchell, R.J. Hilditch)

Principal activities

- SYNROC - examination, dimensioning, density determination, metallography, leaching.
- Moata fuel element inspection
- HIFAR maintenance
- Indium isotope sources
- Gold-labelled sands (isotopes)
- Uranium-doped glass
- Can welding (isotopes)
- Examination of ^{60}Co source
- Loading ^{252}Cf source
- Monitoring ^{60}Co
- Handling nickel hardener spheres

4.4.2 No.2 block

(R.Starling, R.J. Hilditch)

HIFAR flow splitter

A mock-up of a HIFAR flow splitter is being heated to 70°C to simulate reactor conditions with inspections at 1000 h intervals.

Isotope support

The major activity was target transfer, and solid and liquid waste removal manipulator changing in support of ^{99}Mo production.

5. PUBLICATIONS AND CONFERENCE PRESENTATIONS

5.1 Journal Papers

Bowles, J.S., Ball, C.J. and Kelly, P.M. [1982] - On a generalised lattice correspondence theory of martensitic transformations. Scr. Metall. 16:449.

Buykx, W.J., Cassidy, D.J., Webb, C.E. and Woolfrey, J.L. [1981] - Fabrication studies on perovskite, zirconolite, barium aluminium titanate and SYNROC B. Am. Ceram. Soc. Bull., 60:1284.

Reeve, K.D., Levins, D.M., Ramm, E.J., Woolfrey, J.L., Buykx, W.J., Ryan, R.K. and Chapman, J.F. [1981] - SYNROC research and development at Lucas Heights. Aust. Phys., 18:111.

Reeve, K.D., Levins, D.M., Ramm, E.J., Woolfrey, J.L., Buykx, W.J., Ryan, R.K. and Chapman, J.F. [1981] - The development and testing of SYNROC for high-level radioactive waste fixation. At. Energy Aust., 24:2.

Reeve, K.D., Levins, D.M., Ramm, E.J., Woolfrey, J.L. and Buykx, W.J. [1982] - The development and testing of SYNROC as a high-level nuclear waste form. J. Aust. Ceram. Soc., 18:2.

Reeve, K.D., Levins, D.M., Ramm, E.J. and Woolfrey, J.L. [1982] - SYNROC programme progresses. Nucl. Eng. Int., 27:26.

Reeve, K.D., Levins, D.M., Ramm, E.J. and Woolfrey, J.L. [1982] - SYNROC for containment of high-level nuclear waste. Trans. Am. Nucl. Soc., 41:278.

Snowden, K.U., Hughes, D.S. and Stathers, P.A. [1981] - Grain-boundary cavity growth during high-temperature creep and fatigue. Met. Sci., 15:73-78.

Snowden, K.U., Hughes, D.S. and Stathers, P.A. [1982] - The effect of prior fatigue on the creep behaviour of type 321 stainless steel. Int. J. Fatigue 4:217-224.

5.2 Chapter in Book

Snowden, K.U., [1981] - Grain-boundary migration, sliding and void formation during high-temperature fatigue. In Cavities and Cracks in Creep and Fatigue (J. Gittus, ed.). Applied Science Pub., London, Chapter 8, pp.259-289.

5.3 Conference Presentations

Kelly, P.M., Ball, C.J. and Blake, R.G. [1982] - Crystallography of lath martensite in steels. National Conference of Australasian Institute of Metals, Sydney, May.

Levins, D.M., Chapman, J.F., Dale, L.S., Janov, J., Ryan,R.K. and Vilkaitis, V.K. [1981] - The resistance of SYNROC to groundwater attack. 3rd AINSE Engineering Conference, Lucas Heights, November.

Ramm, E.J., Reeve, K.D. and Woolfrey, J.L. [1981] - Status of SYNROC fabrication development. 3rd AINSE Engineering Conference, Lucas Heights, November.

Ramm, E.J. and Reeve, K.D. [1982] - Demonstration of SYNROC fabrication scaleup on non-radioactive basis. Am. Nucl. Soc., Topical Meeting on Treatment and Handling of Radioactive Wastes, Richland, Washington, April.

Ramm, E.J. and Reeve, K.D. [1982] - Demonstration of SYNROC fabrication scaleup using simulated waste. Am. Ceram. Soc., 84th Annual Meeting, Cincinnati, Ohio, May.

Reeve, K.D., Levins, D.M.., Ramm, E.J. and Woolfrey, J.L. [1982] - The development and evaluation of SYNROC for high-level radioactive waste immbolization. IAEA/CEC/NEA International Symposium on the Conditioning of Radioactive Wastes for Storage and Disposal, Utrecht, The Netherlands, June.

Reeve, K.D., Levins, D.M., Ramm, E.J. and Woolfrey, J.L. [1982] - SYNROC for containment of high-level nuclear waste. Am. Nucl. Soc., Annual Meeting, Los Angeles, California, June.

Reeve, K.D., Levins, D.M., Ramm, E.J. and Woolfrey, J.L. [1982] - Immobilization of high-level nuclear wastes in SYNROC. 35th Annual Conference of the Australasian Institute of Metals, Sydney, May.

Reeve, K.D., Levins, D.M., Ramm, E.J., Woolfrey, J.L. and Buykx, W.J. [1981] - The development and testing of SYNROC C as a high-level nuclear waste form. International Symposium on Scientific Basis for Nuclear

Waste Management, Boston, Massachusetts, November.

Reeve, K.D. [1982] - Disposal options of high-level nuclear waste. Australian Drilling Association National Convention, Newcastle, NSW, January.

Ripley, M.I. and Christian, T.W. [1982] - Alloy softening in molybdenum - carbon single crystals. Proceedings of the International Conference on Strength of Metals and Alloys, Melbourne, pp.319-325.

Snowden, K.U., Hughes, D.S. and Stathers, P.A. [1982] - The effect of pre-ageing on the creep behaviour of type 321 stainless steel. Proceedings of the International Conference on Strength of Metals and Alloys, Melbourne, pp.655-663.

Snowden, K.U., Smith, P.D. and Stathers, P.A. [1982] - Effect of specimen size on fatigue crack growth and plastic zone size. Proceedings of the International Conference on Fracture Mechanics Technology, Melbourne (in press).

Woolfrey, J.L., Cassidy, D.J. and Reeve, K.D. [1982] - Irradiation damage effects in SYNROC. Am. Ceram. Soc., 84th Annual Meeting, Cincinnati, Ohio, May.

Woolfrey, J.L., Reeve, K.D. and Cassidy, D.J. [1981] - Accelerated irradiation testing of SYNROC and its constituent minerals using fast neutrons. International Conference on Neutron Irradiation Effects, Argonne, Illinois, November. (in press, J. Nucl. Mater.)

Woolfrey, J.L., Reeve, K.D., Levins, D.M. and Cassidy, D.J. [1981] - Accelerated irradiation testing of SYNROC using fast neutrons. 3rd AINSE Engineering Conference, Lucas Heights, November.

5.4 Patent Applications

Ramm, E.J. and Ringwood, A.E. [1981] - Arrangements for containing waste material. Australia 72825/81; Japan 109533/81; Europe 81303221.6; Canada 382357; USA 282327.